Long-Range Phase-Conjugate Interferometry

Russell M. Kurtz*, Ranjit D. Pradhan, Tin M. Aye, Gajendra D. Savant, and Tomasz P. Jannson
Physical Optics Corporation, Torrance, CA 90501
Marvin B. Klein
Lasson Technologies, Inc., Culver City, CA 90230

ABSTRACT

The most accurate method of measuring distance and motion is interferometry. This method of motion measurement correlates change in distance to change in phase of an optical signal. As one mirror in the interferometer moves, the resulting phase variation is visualized as motion of interferometric fringes. While traditional optical interferometry can easily be used to measure distance variation as small as 10 nm, it is not a viable method for measuring distance to, or motion of, an object located at a distance grater than half the coherence length of the illumination source. This typically limits interferometry to measurements of objects within <1 km of the interferometer. We present a new interferometer based on phase conjugation, which greatly increases the maximum distance between the illumination laser and the movable target. This method is as accurate as traditional interferometry, but is less sensitive to laser pointing error and operates over a longer path. Experiments demonstrated measurement accuracy of <15 nm with a laser-target separation of 50 times the laser coherence length.

1. INTRODUCTION

Extremely accurate distance and motion measurements have been important in the laboratory, and are now becoming more important for experiments outside the laboratory. NASA, for example, is developing separated-spacecraft interferometry (Fig. 1), in which two spacecraft must be held in the same relative position—to within a few microns—for long enough to view distant objects. These spacecraft may be separated by tens of kilometers, yet their relative motion must be known. The state of the art in nanomotion measurement (measurement of motion at <1 μm/s or distance variation of <1 μm) is heterodyne optical interferometry, which can measure displacements as small as 20 pm in carefully controlled laboratory situations[1] and motion of 10 nm/s in ordinary laboratory conditions. These results have been demonstrated at laser-target separations as large as 600 m, using line-narrowed lasers whose coherence length exceeded 1,500 m. Such high-quality lasers were necessary because optical interferometry only operates over distances that do not exceed half the laser coherence length. This limits the usefulness of heterodyne optical interferometry in space, since the spacecraft separation can be 50 times the coherence length of the best space-qualifiable laser.

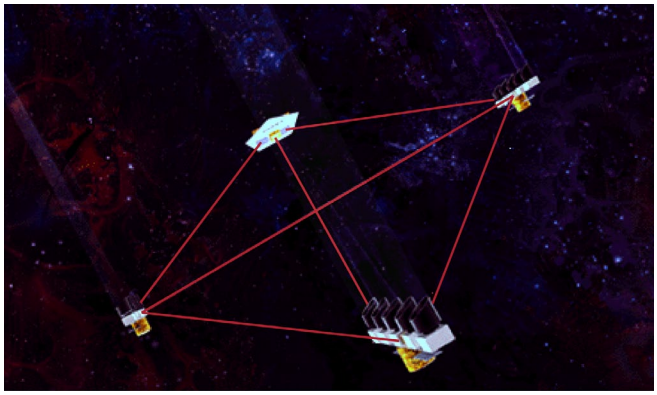

Fig. 1. A tetrahedral arrangement of separated spacecraft for very long distance interferometry. The spacecraft are locked together by motion measurement and feedback.

* rkurtz@poc.com, phone 1 310 320-3088, fax 1 310 320-4667, www.poc.com

Spaceborne Sensors, edited by Robert D. Habbit, Jr., Peter Tchoryk, Jr.,
Proceedings of SPIE Vol. 5418 (SPIE, Bellingham, WA, 2004)
0277-786X/04/$15 · doi: 10.1117/12.543824

One application of separated-spacecraft interferometry is the search for planets around distant stars. To see the Earth as an object separate from the Sun, for example, an observer at the center of our galaxy would require an interferometer with a baseline of nearly 20 km. To resolve a planetary system in the Andromeda galaxy from the Solar System would require a separated-spacecraft interferometer whose baseline is greater than 300 km. Since the separation between spacecraft is so large, heterodyne optical interferometry would not be successful. Laser radar is another method of measuring distances, but its accuracy is much lower than interferometry. With pulsed laser radar, it is difficult to measure distances less than a few millimeters. The uncertainty principle limits laser radar accuracy to $\lambda/2\pi$, where λ is the wavelength of the illumination laser; real-world accuracy is much lower. Thus, a new method of measurement is needed if nanomotion is to be determined at distances greater than ~1 km. Such a method—long-range phase-conjugate interferometry—is presented in this paper. Preliminary experiments have demonstrated measurements of distance accurate to 15 nm and motion of 290 nm/s in the laboratory, accuracy only achievable by interferometric measurements, even at distances 50 times the coherence length of the laser. Calculations demonstrate that this accuracy can be maintained at distances up to 8,000 km (four orders of magnitude greater than the state of the art).

2. THEORY

The theory behind long-range phase-conjugate interferometry can be divided into three parts: motion and displacement measurement by interferometry, improvements by phase conjugation, and applications to long-range measurement.

2.1. Interferometry

Interference is a result of the wave nature of light, and has been known for nearly 350 years[2]. It is a measure of the coherence of light, and occurs when two beams that are nearly monochromatic, at approximately the same frequency, and with similar polarization are mixed together in a nearly collinear orientation[3]. To describe interference, it is necessary to describe light in terms of an electromagnetic field. Specifically, the electric field of a propagating beam at a given point in space can be described as

$$E_1(x, t) = A_1\cos(kx - \omega t) \ , \tag{1}$$

where A_1 is a real constant, E_1 is the real electric field, $k = 2\pi/\lambda$ is the wavenumber, λ is the wavelength of the light, $\omega = kc$ is the radian frequency (2π times the frequency), and c is the speed of light. Eq. (1) describes a beam propagating in the x direction and polarized in the z direction. Another beam might be described by

$$E_2(x, t) = A_2\cos(kx - \omega t + \varphi) \ , \tag{2}$$

a beam propagating identical to beam 1 but with constant phase difference φ. These beams are collinear. For optimum contrast the two beams must have the same amplitude, so we set $A_1 = A_2 = 1$. Then the sum of the electric fields can be written

$$E_1(x,t) + E_2(x,t) = 2\cos\left(kx - \omega t + \varphi/2\right)\cos\left(\varphi/2\right) \ . \tag{3}$$

In other words, the sum of the two fields is twice the original field, phase shifted by half the phase difference between the fields and multiplied by the cosine of half the phase difference between the fields. Detectors (and eyes) do not detect the electric field directly, but detect the intensity, which is a constant times the square of the electric field. The intensity is a constant multiplied by the square of the field. In the special case in which the phase difference is 0, the sum of the fields is simply twice the field; when the phase difference is 180°, the sum of the fields is 0; and when the phase difference is ±90°, the sum of the fields is constant with the amplitude of one field. Intensities, as would be seen by a detector, camera, or the eye, are plotted in Fig. 2.

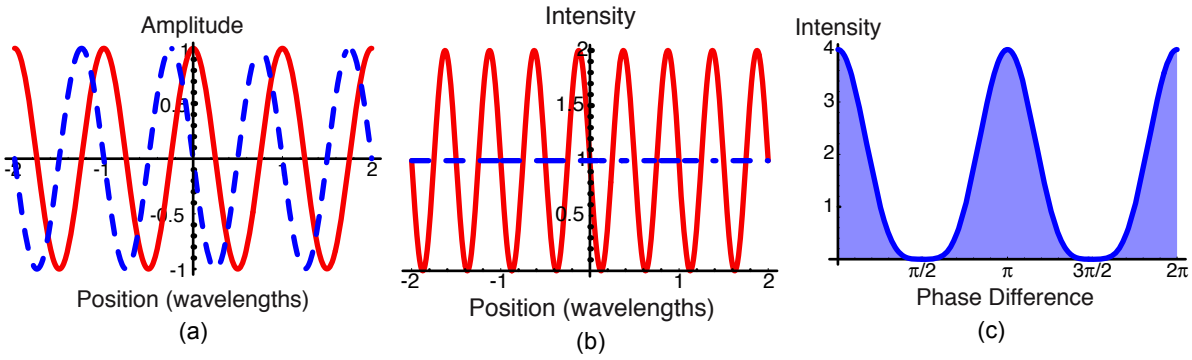

Fig. 2. Intensities and electric fields described above. The amplitude of E_1 (solid) and E_2 (dashed) are shown in (a). If the phase difference between the two beams is 90°, the incoherently added intensity of the beams is constant (b – dashed line), while the coherently added intensity depends on position (b – solid line). The average intensity of the combined beam depends on the phase difference between the two beams (c).

The intensity of the beam shown in Fig. 2(b) demonstrates that the average intensity at most phase differences varies with position, but the plot is somewhat misleading. The units are wavelengths of light, so the variation is too small to see. What the detector, camera, or eye actually sees is the average intensity, which is the same in Fig. 2(b) for incoherent and coherent addition. This situation only occurs for a phase difference of 90° (or $\pi/2$ radians). The average intensity as a function of phase difference between the beams is plotted in Fig. 2(c), which shows how interference results in fringes.

The equations for interference are relatively simple for collinear beams. The intensity of the beams, within a constant factor, are

$$I_1(x,t) \equiv E_1^2(x,t) = \cos^2(kx - \omega t) = \frac{1}{2} + \frac{1}{2}\cos\left[2(kx - \omega t)\right] \tag{4a}$$

and

$$I_2(x,t) \equiv E_2^2(x,t) = \cos^2(kx - \omega t + \varphi) = \frac{1}{2} + \frac{1}{2}\cos\left[2(kx - \omega t + \varphi)\right] \quad . \tag{4b}$$

The intensity of the sum of the beams is

$$I_{tot}(x,t) \equiv \left(E_1(x,t) + E_2(x,t)\right)^2 = 1 + \cos(2\varphi) + \{\cos(kx - \omega t)^n \text{ terms}\} \quad . \tag{5}$$

Eq. (5) can be broken into three parts: one that varies with a period of half the wavelength of light and/or at a very high frequency, one that is constant, and another that is constant over distance (but depends on the phase difference between the two beams). The parts that vary over small distances or at high frequencies average to 0, leaving us with a visible average intensity of

$$I_{avg} = 1 + \cos(2\varphi) \quad . \tag{6}$$

This is a periodic equation in φ whose magnitude varies from 0 to 2.

In this perfectly aligned case, the intensity is dependent only on the phase difference between the two beams. This phase difference can be altered by changing the propagation path between the two beams, in (for example) a Michelson interferometer (Fig. 3).

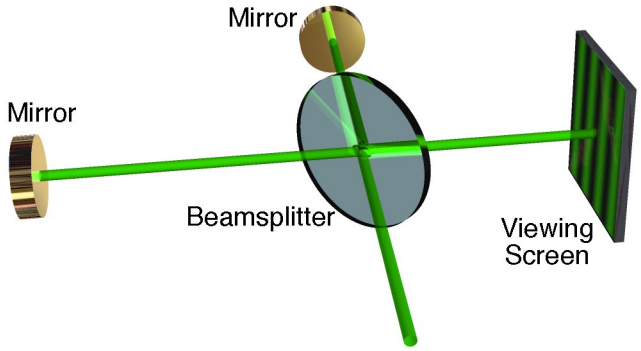

Fig. 3. Layout of a Michelson interferometer. An incoming laser beam is split by a beamsplitter. Each beam is retroreflected by a mirror. They are recombined at the beamsplitter and directed onto a viewing screen that shows an interference fringe pattern representing the differences between the two beams. When one mirror moves axially, the fringe pattern shifts.

If the two mirrors of a Michelson interferometer are aligned perfectly, the resulting fringe pattern has a period that is nearly infinite. Then the only phase change is caused by movement of one of the mirrors along the optical axis. The interference pattern varies from dark to light and back to dark as the moving mirror translates through 1/4 of the laser wavelength. The intensity varies with translation distance as shown in Fig. 2(c), where 1/4 wavelength corresponds to 2π phase difference. Interferometry is the most accurate method known of measuring distance. Since 1/8 wavelength mirror motion corresponds to complete variation from light to dark, if a detector can measure (for example) 250 levels in its response to this input, the interferometer could detect displacement of 1/2,000 the laser wavelength. Using blue light at 400 nm, such an interferometer would be capable of distance measurements with an accuracy of 200 pm. By measuring over a long period of time with more accurate detectors, scientists have exceeded this accuracy by a factor of 10 in the laboratory[1].

Note, however, that the calculations in Eqs. (1-6) have assumed the two beams were exactly collinear and had exactly the same wavelength – that the only difference between them was phase. This is true for lasers approximately over their coherence length (which is proportional to the inverse of their bandwidth). Laser coherence length can vary widely depending on the type of lasers and on the laser cavity. Simple semiconductor lasers, for example, often have coherence lengths of about 1 mm (LED coherence lengths are in the micron range); the best commercial holography lasers have coherence lengths exceeding 1 km. Line-narrowing by means of gratings and etalons increases the coherence length of a commercial argon laser from <3 cm to >100 m. Since an interferometer for distance measurement requires a beam to propagate to the target, be reflected, and return, the total propagation distance from the illumination laser to the detector is twice the distance to the target, limiting traditional interferometry to targets that are separated by less than half the laser coherence length. It is possible to increase this slightly by inserting an optical delay in the non-propagating beam, but the optical delay line can introduce additional complications. Generally, optical interferometry is performed only over a distance of half the coherence length of the laser.

2.2. Phase conjugation

2.2.1. Review of theory

Phase conjugation in long-range phase-conjugate interferometry is an effect of four-wave mixing in a nonlinear material. We again assume the beams are collinear; the approximate layout is shown in Fig. 4. The pump beams are counterpropagating:

$$E_1(x, t) = A_1\cos(kx - \omega t) \quad \textit{forward pump} \tag{7a}$$

$$E_2(x, t) = A_2\cos(kx + \omega t) \quad \textit{backward pump} \ . \tag{7b}$$

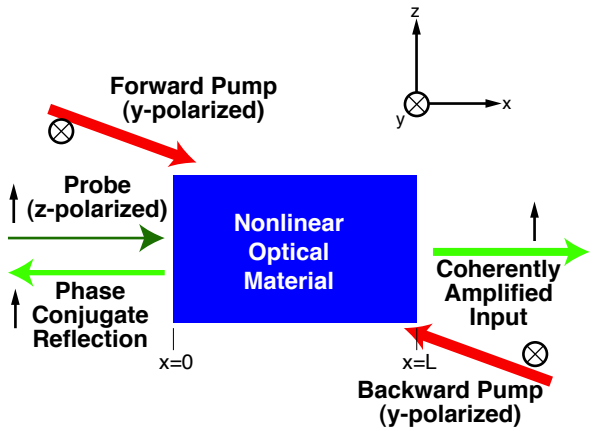

Fig. 4. Propagation and polarization of beams in four-wave-mixing phase conjugation. The forward and backward pump beams are approximately collinear with the probe beam.

A third beam, called the probe, is added to the two pumps. The pump beams are polarized in the y direction, but the probe is polarized in the z direction. For simplicity we model the three beams as being collinear. The probe is described by

$$E_3(x, t) = A_3\cos([k+\Delta k]x - [\omega+\Delta\omega]t) \quad probe \ . \tag{8}$$

The nonlinear material has a susceptibility χ_{zyyz} that describes the nonlinear polarization created, polarized in the z direction, by two pump beams polarized in the y direction and a probe beam polarized in the z direction. This nonlinear polarization is proportional to the product of the three beams:

$$P_{NL}(x, t) = 4\,\chi_{zyyz}\,A_1\cos(kx - \omega t)\,A_2\cos(kx + \omega t)\,A_3\cos([k+\Delta k]x - [\omega+\Delta\omega]t) \tag{9a}$$

$$= 2\,\chi_{zyyz}\,A_1A_2A_3[\cos(2kx) + \cos(2\omega t)]\cos[(k+\Delta k)x - (\omega+\Delta\omega)t] \ . \tag{9b}$$

The terms cos(2kx) and cos(2ωt) are stationary and vary through cycles less than a wavelength of the beams. We view them as averages, and each averages out to 1/2. The nonlinear polarization is thus

$$P_{NL}(x, t) = 2\,\chi_{zyyz}\,A_1A_2A_3\cos[(k+\Delta k)x - (\omega+\Delta\omega)t] \ . \tag{10}$$

This nonlinear polarization field generates a fourth wave which, to conserve momentum and energy, is

$$E_4(x, t) = 2\,\chi_{zyyz}\,A^*_1A^*_2A^*_3A_4\cos[(k-\Delta k)x + (\omega-\Delta\omega)t] \ , \tag{11}$$

where A_4 is a purely real constant. The pump beams are generally split from one originating beam and are of equal power counterpropagating; thus,

$$A_1 = A^*_2 \ . \tag{12}$$

Thus, Eq. (11) can be rewritten

$$E_4(0, t) = A_TE^*_3(0, t) \ , \tag{13a}$$

where

$$A_T = 2\,\chi_{zyyz}\,A_4|A_1|^2 \ . \tag{13b}$$

E_4 is thus a real constant multiplied by the complex conjugate (phase conjugate) of E_3. But what is this constant? Yariv and Yeh[4] derive the constant to be

$$A_T = \tan(\kappa L) \ , \tag{14a}$$

where

$$\kappa = \frac{3}{2}\omega\sqrt{\frac{\mu}{\varepsilon}}\chi_{zyyz}|A_1|^2 \quad , \tag{14b}$$

L is the interaction length within the crystal, μ is the linear magnetic susceptibility of the nonlinear material, and ε is the linear dielectric permeability of the nonlinear material. For an estimate of the value of A_T, which is the gain of the phase conjugate reflection with respect to the probe, Eq. (14b) is first rewritten in terms of pump intensity as

$$\kappa = \frac{12\pi\chi_{zyyz}}{n^3\varepsilon_0^2 c\lambda} I \quad . \tag{14c}$$

In Eq. (14c), n is the refractive index of the nonlinear material for the polarization of the probe and ε_0 is the permeability of free space. As an example, assuming a 1 cm interaction length, pump intensity of 35 MW/cm^2, and interaction in KDP[5] (n = 2.25 and $\chi_{zyyz} = 3.0\text{x}10^{-28}$ F cm/W-Ω), the expected phase conjugate gain of the modeled system is

$$A_T = \tan(\kappa L) = 5.5 \quad . \tag{15}$$

This pump intensity is easily reached with a small mode-locked pump laser. Clearly, the phase conjugate gain can be adjusted by varying either the interaction length or the pump intensity. For example, keeping the same pump intensity, increasing the interaction length to 1.1 cm increases the gain by more than a factor of 4, to 24. Alternatively, reducing the pump beam intensity from 35 MW/cm^2 to 25 MW/cm^2 reduces the gain by a factor of approximately 3.5, to a gain of 1.5.

Referring again to Fig. 4, the coherently amplified input must be described. Eq. (13a) shows that the reflected beam (at x = 0) is the gain multiplied by the phase conjugate of the probe (at x = 0). But there is no phase conjugate beam for x > L. By the same calculations that lead to Eqs. (14), the nonlinear polarization amplifies the forward-propagating probe. Conservation of energy demands that this amplified beam be the exact phase conjugate of the reflected beam, even in terms of power. Additionally, the probe beam energy must be included. These calculations result in an output that is coherent with the probe, with gain $A_T + 1$. In other words,

$$E_3(L,t) = (A_T + 1)E_3(0,t) = \frac{A_T + 1}{A_T} E_4^*(0,t) \quad . \tag{16}$$

2.2.2. Interpretations for interferometry

Eq. (16) makes clear that the pump and the amplified probe are mutually coherent beams. Thus, they will interfere with each other as described in Section 2.1. The ratio of the gains of these two beams shows that the amplified probe will always be more powerful than the phase conjugate reflection. Nonetheless, for large gain ($A_T \gg 1$), the two beams will have nearly the same intensity. They can interfere with high contrast and form an easily readable interference pattern. High gain has been reported[6] in many experiments involving a gain medium as the nonlinear material. If $A_T \approx 100$, for example, there will only be about a 1% difference between the amplified probe and the phase conjugate reflection.

Another effect of phase conjugation is frequency reversal. Comparing Eqs. (8) and (11), any frequency shift in the probe is matched by the opposite frequency shift in the phase conjugate beam. This shows up in two effects: if the center wavelength of the probe is slightly shifted from the center wavelength of the pumps, the center wavelength of the phase conjugate reflection will be shifted by an equal amount in the opposite direction; and if the frequency distribution of the probe is asymmetric, the phase conjugate frequency distribution will be the mirror image of the probe. This is illustrated in Fig. 5.

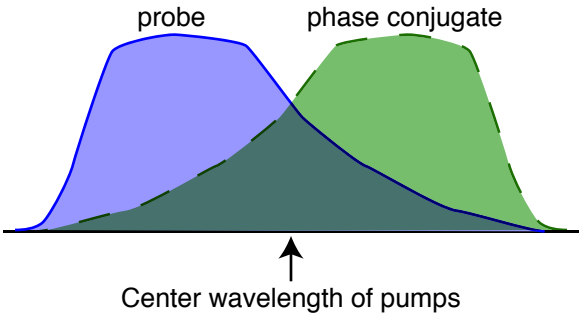

Fig. 5. Illustration of the frequency reversal property of phase conjugation.

2.3. Motion detection through Doppler shift

Motion can be detected by means of a Doppler shift. This shift occurs when the target is in motion with respect to the illuminator. The axial component of relative motion (the component along the axis connecting the illuminator and the target) v_A, introduces a frequency shift in the incoming signal of

$$\Delta f = -v_A/\lambda \ , \tag{17}$$

where λ is the wavelength of the incoming light. The frequency reversal property of phase conjugation makes it clear that any Doppler shift in the probe will also appear in the phase conjugate reflection, but with the opposite sign. This is the basis of motion detection through interferometric measurement of the Doppler shift. If the incoming signal, with the Doppler frequency shift, is mixed with a signal at the same wavelength but lacking the Doppler shift, the resulting interference pattern will have a beat frequency equal to the Doppler frequency. The output will display a temporal pattern similar to that in Fig. 2(c), where $1/\Delta f$ replaces 2π. If the phase conjugate reflection is mixed with the coherently amplified probe, the frequency difference between the two will be twice the Doppler shift. Thus, the beat frequency observed if these two signals are mixed is twice the Doppler frequency. By observing the interference pattern, which oscillates at four times the Doppler frequency, relative velocity can be calculated. The velocity is then integrated to measure the distance displacement. Distance measurement resolution is limited by the capability of the detector system to determine changes in the brightness of the signal falling on it.

2.4. Applications to long-range interferometry

Phase conjugate interferometry has two major advantages over traditional optical interferometry (including heterodyne optical interferometry) when it comes to long-range applications. The first is that the effects of propagation are greatly reduced. For example, if the target is 10 km away from the illuminator, traditional interferometry requires the illumination beam to travel a total of 20 km – to the target and back. The phase conjugate interferometric system can be placed on the target, reducing the propagation distance to 10 km (although other factors may lead to placing the phase conjugate system with the illuminator). When the phase conjugate gain is considered as well, it is clear that the separation between the illuminator and the target can be significantly greater for a phase conjugate system than for tradition interferometry.

Even more significant is the reduction in coherence requirements. A phase conjugate interferometer (Fig. 6) can be relatively small, and the interfering beams only travel the distance around the interferometer after being split. In other words, the distance between the illuminator and the target no longer has any effect on the coherence requirement of the interferometer. Additionally, since the reflected beam is the phase conjugate of the amplified probe, it is effectively traveling backwards. A beam will be coherent with its phase conjugate reflection over a range much greater than its coherence length.

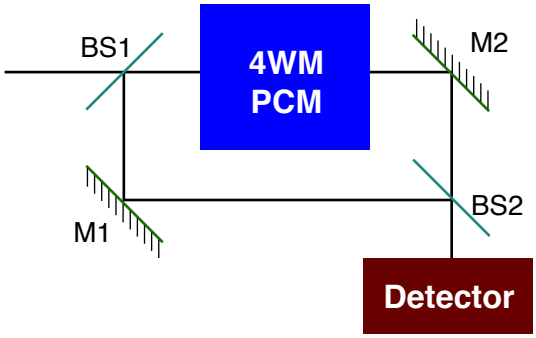

Fig. 6. Conceptual layout of a phase conjugate interferometer. The incoming probe beam passes through beamsplitter BS1 and into phase conjugate mirror PCM. The probe is amplified coherently by four-wave mixing (4WM), is reflected by mirror M2, and passes through beamsplitter BS2 to reach the detector. The phase conjugate beam reflects from beamsplitter BS1 and is directed by mirror M1 to beamsplitter BS2, where it is combined with the amplified probe and directed onto the detector. The interference pattern between the probe and phase conjugate signals is the output of this interferometer.

Calculating the maximum useful distance between the illuminator and the target is equivalent to specifying the illumination laser. Its requirements depend on three items: required spectral purity, intensity needed to excite the detector, and beam divergence (which is related to the pointing accuracy requirement). Traditional optical interferometry requires a laser that is spectrally very narrow. This is a result of the need to maintain the separation between the target and the illuminator to less than the coherence length of the laser. The coherence length is inversely proportional to the laser spectral bandwidth. The relationship is

$$x_C < c/\Delta\nu, \tag{18}$$

where x_C is the coherence length, $\Delta\nu$ is the laser spectral bandwidth, and c is the speed of light. As described above, these requirements are greatly reduced by a phase conjugate interferometer. Coherence lengths as short as a few millimeters are acceptable.

The illumination laser power required to generate a response from a photodetector can also be calculated. A typical photodetector has a response of 10 μV/photon which, for a 2 mm^2 detector and 1.064 μm laser illumination, is 17.8 V/(nW/cm^2). Thus, to achieve an output of 100 mV, the detector must see an intensity of 5.6 pW/cm^2. (This is below the cosmic background radiation level of 313 pW/cm^2. An interferometer, however, has a bandwidth that is very small compared to the cosmic background radiation, so that detectors see extremely low background intensities.) Using a telescope with a 10 cm aperture and a 1 cm output, this intensity is reached when the illumination laser intensity at the target is 0.056 pW/cm^2. In a typical Michelson-based phase conjugate interferometer (as illustrated in Fig. 6), the probe experiences a loss of 50% before phase conjugation, and another 50% afterwards. Even with a phase conjugate reflectivity as low as 1%, then, the output from the detector is useable if the illumination laser intensity is 30 pW/cm^2.

Beam divergence is related to both illumination laser intensity at the target and required pointing accuracy. The tradeoff is due to the fact that the wider the beam, the lower the average intensity, but the higher the relative intensity at a given angle off axis. The intensity of a beam characterized by beam quality parameter M^2 at a distance x from the original laser output is

$$I(x) = I_0 \frac{A_0}{A_0 + M_0(x)} \mathrm{Exp}\left(-\pi r^2 \frac{A_0}{A_0^2 + M_0^2(x)}\right), \tag{19}$$

where r is the distance off axis, I_0 is the intensity at the laser beam waist (which may be within the laser cavity, in which case I_0 is the intensity at that point multiplied by the transmission of the output coupler), the beam diameter at the waist is d_0, and A_0 and $M_0(x)$ are parameters defined by

$$A_0 \equiv \frac{\pi d_0^2}{4}, \tag{20a}$$

$$M_0(x) \equiv x\lambda\sqrt{M^2} \quad . \tag{20b}$$

The relative intensity ($I(x)/I_0$) as a function of illumination laser pointing error and beam quality is shown in Fig. 7. This figure demonstrates that a higher value of M^2 leads to lower intensity on axis, but higher intensity off axis. This figure does not vary significantly with illuminator-target distance (as long as this distance is large compared to the beam diameter).

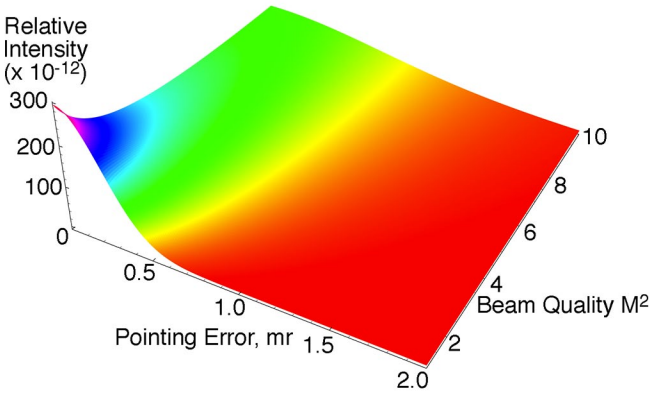

Fig. 7. Relative intensity of the illumination laser as a function of pointing error and beam quality. Lower beam quality (higher M^2) permits greater pointing error for the same level of relative intensity, but also results in lower absolute intensity.

Eq. (19) can be solved to find that a 1 W Nd:YVO_4 illumination laser with a beam diameter of 2 mm and M^2 of 5, propagating 100 km, still produces 0.1 nW/cm^2 at the target for an off-axis angle of nearly 4 mr. Reducing the distance between the illuminator and the target increases this permissible pointing error only slightly, while increasing the illumination laser power to 10 W increases the permissible pointing error to over 5 mr. One result of these calculations is that a lower quality beam permits greater pointing error, but requires a more powerful laser.

The above calculations demonstrate that, even if the phase conjugate gain is very low or if the illumination beam must propagate over an entire round trip (to the target and back), phase-conjugate interferometry can be used for motion measurements even for target-illuminator separations of over 100 km. If we increase the gain to 150, the maximum distance between the illuminator and the target can reach 8,000 km, with pointing accuracy requirements of ~2 mr.

3. EXPERIMENT

A laboratory experiment was performed to demonstrate long-range phase conjugate interferometry (Fig. 8). Light from an argon laser operating at 514.5 nm passed through a beamsplitter. The 10% reflected served as the probe. The argon laser has a bandwidth of ~10 GHz, corresponding to a coherence length of 3 cm (Eq. (18)). The light that passed through the beamsplitter was again split, this time into the forward and backward pump beams. The forward pump was approximately twice as powerful as the backward pump, which optimized the reflectivity in the Cu:KNSBN nonlinear crystal. Care was taken to align all beams so as to avoid any self-pumped photorefractivity in this crystal. The probe was directed towards the crystal initially by a mirror on a piezoelectric stack, which had a maximum motion of 17 μm. This beam entered the crystal at an angle such that it intercepted the counterpropagating pumps at an angle of ~90°. The distance from the piezo mirror to the nonlinear crystal was 150 cm, or 50 times the coherence length of the argon laser. A beamsplitter was placed in the probe between the last mirror and the Cu:KNSBN crystal. This formed a Michelson interferometer, with the input being the last mirror to the beamsplitter, one leg between the beamsplitter and the external mirror, and the other leg between the beamsplitter and the phase conjugate mirror, all observed at the detector. Driving the piezoelectric stack introduced motion between the probe and the phase conjugate mirror. Two detectors were included in the setup. First a CCD camera visualized interferometric fringe motion. The second, more accurate detector, was a photodetector placed behind a beam expander. This detector produced a voltage output

proportional to the light striking it. As the piezo mirror moved, the interferometric fringes appeared to move, producing a sinusoidal voltage output from the photodetector.

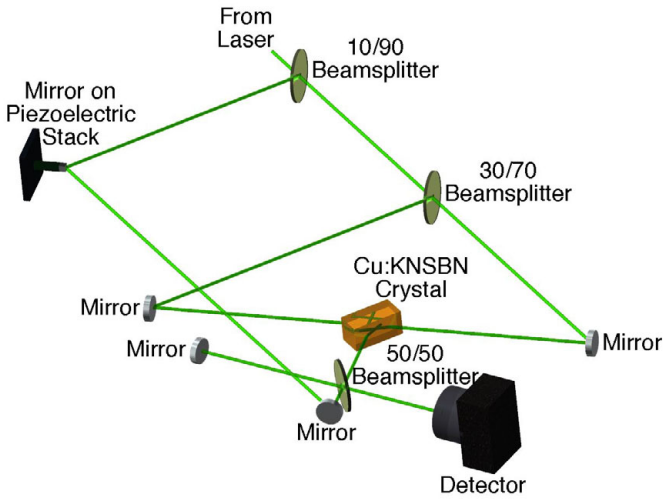

Fig. 8. Layout of the phase-conjugate interferometry experiment.

The first step in the experiment was to calibrate the motion of the piezoelectric stack by traditional optical interferometry. With the piezo mirror as one mirror in a Michelson interferometer, the stack was driven with a triangle wave from a function generator, amplified to 40 V. The results are shown in Fig. 9.

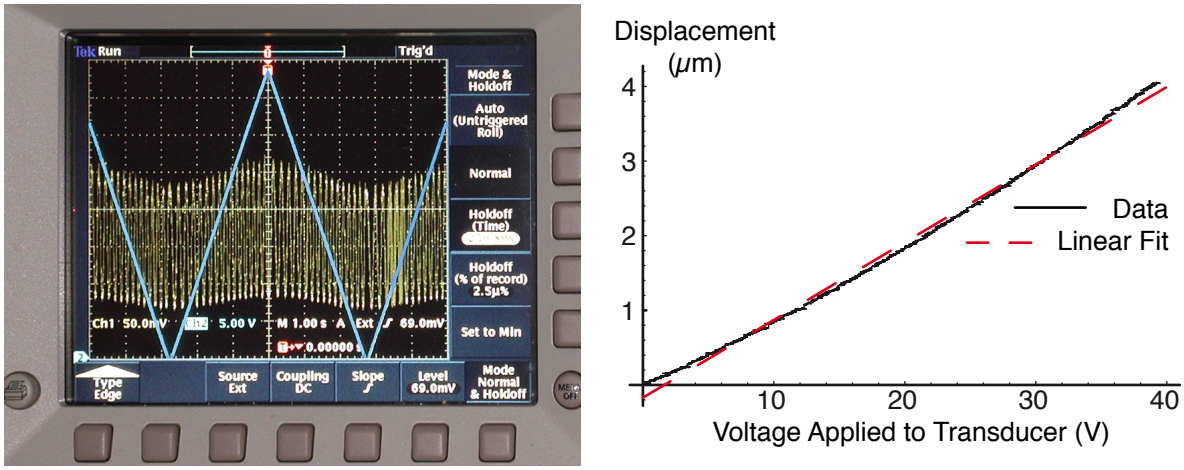

(a) (b)

Fig. 9. Calibration of the piezoelectric stack. A mirror mounted on the stack functions as the movable mirror in a Michelson interferometer. Motion of the mirror appears as motion of the interferometric fringes. The voltage applied to the piezoelectric transducer (a – slower motion) and the fringe brightness (a – rapid variation) are combined to form the displacement vs. voltage curve (b – solid black curve). A best linear (b – dashed curve) fit was also calculated.

The displacement of the piezoelectric transducer is fit extremely well (RMS error = 0.032%) by a quadratic equation,

$$x = \frac{V^2}{1616} + \frac{2V}{25} - \frac{1}{90} \quad , \tag{21}$$

where x is the displacement (µm) of the mirror at the end of the piezoelectric stack and V is the voltage (V) applied to the stack. As seen in Fig. 9(b), the motion is also fit well (RMS error = 0.14%) by a linear equation,

$$x = \frac{5V}{48} - \frac{8}{47} \quad . \tag{22}$$

Despite the low RMS error of the linear model, the quadratic model was used as the calibration equation for the piezo mirror motion.

Fig. 10 shows apparent motion of the fringe as a function of relative motion of the probe mirror. The straight line represents the predicted motion equation,

$$f_f = 3.95\ v \quad , \tag{23}$$

where f_f is the frequency of the signal measured by viewing one point on the interference pattern with a photodetector (Hz) and v is the measured relative velocity of the mirror mounted on the piezoelectric stack (μm/s). Relative motion of the mirror is easily measured by determining the fringe frequency.

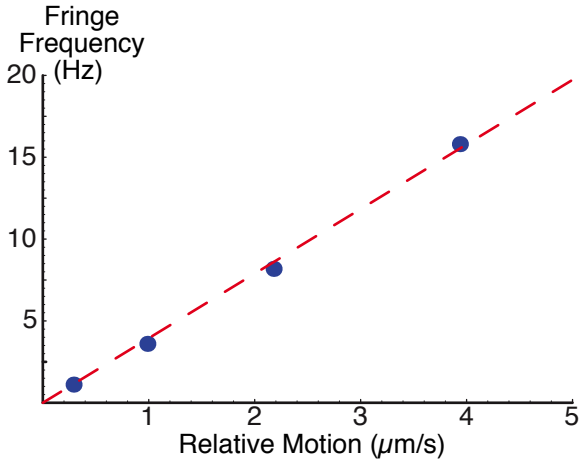

Fig. 10. Demonstration of long-range phase conjugate interferometry for measuring motion. Dashed line is the predicted relationship between velocity of the piezo mirror and fringe variation frequency; dots are actual measurements.

The output from the photodetector is a sinusoidal function of the phase difference between the two arms of the Michelson interferometer. As such, it moves from minimum to maximum as the piezo mirror moves one-eighth wavelength (~64 nm in this experiment). In the phase conjugate interferometry experiment, the photodetector output was digitized, and the inverse sine function was applied to result in the wrapped phase (modulo 2 π). These calculated values were then unwrapped, directly resulting in displacement values. To generate the values of Fig. 10, the raw signal was digitized and the frequency of zero-crossing was calculated. Half this frequency was the fringe frequency. The period of the triangle wave drive signal and its amplitude (Fig. 9(a)) were also digitized and calibrated according to Eq. (21). These results determined the speed of the piezo mirror motion.

4. CONCLUSIONS

Long-range phase-conjugate interferometry has been shown to have many of the advantages of traditional optical interferometry, including the heterodyne methods that have been used to measure displacements as small as 20 pm in the laboratory. Calculations show that it can be used at illumination-target separations four orders of magnitude greater than traditional interferometry, with no loss of resolution, by designing the interferometer so as to reduce the optical path difference between the two arms to a few mm. A phase conjugate interferometry experiment was performed over a distance 50 times the coherence length of the illumination laser—two orders of magnitude greater than the maximum range of traditional interferometry—to demonstrate the advantages of phase conjugate interferometry. This experiment measured motion of a mirror mounted on a piezoelectric stack. The experimental setup proved capable of measuring motion as small as 15 nm and velocity as low as 290 nm/s, limited by the equipment and not by the technique. Calculations show the experimental system to be capable of detecting displacement as small as 200 pm. The improvements inherent in phase-conjugate interferometry recommend its use in separated-spacecraft experiments and

other situations where the nanomotion variation between two separated items must be measured, and the separation is greater than half the coherence length of the illumination laser.

ACKNOWLEDGEMENTS

The authors gratefully acknowledge NASA-JPL for its support of this work under SBIR contract NAS-03069.

REFERENCES

1. "Interferometer for Measuring Displacement to Within 20 pm," *Phot. Tech. Briefs*, 8a-9a, 2003.
2. R. Hooke, *Micrographia*, 1665.
3. J. Tervo, T. Setälä, and A.T. Friberg, "Degree of Coherence for Electromagnetic Fields," *Opt. Exp.*, **11**, 1137-1143, 2003.
4. A. Yariv and P. Yeh, *Optical Waves in Crystals*, John Wiley & Sons, New York, 1984.
5. F. Zernicke and J.E. Midwinter, *Applied Nonlinear Optics*, John Wiley & Sons, New York, 1972.
6. T. Omatsu, B.A. Thompson, A. Minassian, and M.J. Damzen, "150-Times Phase Conjugation by Degenerate Four-Wave-Mixing in a Continuous-Wave Nd:YVO_4 Amplifier," *OSA/IEEE Conference on Lasers and Electro-Optics*, vol. 73, 207-208, Long Beach, California, 2002.